

Network Formation in a Crystallizing Polymer

Deepak Arora¹ and H.Henning Winter^{1,2}

¹Department of Polymer Science and Engineering, University of Massachusetts Amherst, Amherst, MA 01003

²Department of Chemical Engineering, University of Massachusetts Amherst, Amherst, MA 01003

INTRODUCTION

The spherulitic growth of crystals in a semicrystalline polymer is initiated by lowering the temperature from the melt stage. Below a polymer-specific temperature level, nuclei begin to appear. On these nuclei, lamellar crystals grow to form spherulitic structures, followed by their impingement. The impingement of spherulites gives rise to grain boundaries in a semicrystalline polymer. As a consequence of crystallization, the material undergoes a liquid-to-solid transition, which can be captured by rheological gel point measurements. Dynamic mechanical spectroscopy (DMS) is a very sensitive tool to locate the gel point which expresses itself in a self-similar relaxation modulus, $G(t) = St^n$ for $t > 1/\omega_c$. In case of dynamic mechanical measurements, the gel point structure results in complex moduli $G^* = G' + iG'' = S\Gamma(1-n)\cos(n\pi/2)\omega^n$, and a frequency independent loss tangent, $\tan\delta = \tan(n\pi/2) \neq f(\omega)$ for $\omega < \omega_c$, in the terminal region. S is the gel-stiffness and n is the relaxation exponent for the critical gel. For crystallizing homopolymers, the mechanism that causes the fluid-to-solid transition is not well-understood². The objective of this work is to identify the connectivity mechanism and, specifically, to identify the structure at the gel point.

EXPERIMENTAL

Material and Sample Preparation. Isotactic poly-1-butene (iPB), from Basell, with $M_w = 176000$ and M_w/M_n of 5.7, served as test material. The iPB was used without a nucleating agent. For the DSC measurements (DSC Q1000, TA Instruments), samples were heated as well as cooled at 10K/min. First melting, second melting, and crystallization peaks were observed at 120 °C (100-130 °C), 110 °C (100-120 °C), and 54 °C, respectively (Fig. 1). First melting belongs to the crystal FormI of iPB, which has a density of 950 Kg/m³ and is a thermodynamically stable form. Second melting belongs to FormII that is less dense (907 Kg/m³) than FormI and is a kinetically favored crystal form. FormII transforms into FormI within 7-12 days at room temperature and atmospheric pressure³.

For rheology, a 2mm thick disk-shaped sample was inserted between the parallel disk fixtures (diameter 25 mm) of a torque-controlled rheometer (Stresstech of ATS Rheosystems). It was heated above melting point and then compressed to a thickness of about 0.9 mm to establish uniform contact between the sample and rheometer plates. G^* - G'' data from isothermal frequency sweeps at $T = 88.9, 100.8, 110.9, 121.4, 131.5, 141.5, 151.8,$ and 174 °C were merged into a master curve at 88.9 °C (Fig. 2). The shear measurements were performed in the linear viscoelastic region. For cross-polar microscopy, a 2 mm thick disk shaped sample was placed between the parallel plates of an optical device (CSS 450 from Linkam Scientific). There, it was heated above melting and then compressed to a thickness of about 300 μ m.

Experimental Protocol. For all the experiments, samples were heated to 174.5 °C, kept there for about 15 minutes. Such a high temperature (about 50 K above melting) was used to erase the thermo-mechanical history as recommended by Hadinata *et al.*⁴. Then the sample was cooled down to $T_x = 88.9$ °C, the temperature for isothermal crystallization. Time $t = 0$ was assigned to the instant at which the experimental temperature T_x was reached.

RESULTS

Rheology. The purpose of the rheological experiments is to find the gel point so that the structural properties can be measured at that transition. Figure 3 shows the respective development of the storage

(G') and loss (G'') moduli. Both moduli grow with time and level off at longer times. It was surprising to observe the frequency independence of plateau values at longer times for both the moduli. However, this trend is not unique, glassy materials demonstrate similar behavior⁵.

The gel point as marked by a loss tangent that is independent of frequency¹ can be measured with time-resolved oscillatory shear¹ at frequencies between 0.1 and 0.8 rad/s. The loss tangent was found to intersect at $t_{gel} = 1180-1192$ s (Fig. 3). Gel stiffness and relaxation exponent are $S = 1.85-2.54 \times 10^4$ Pa sⁿ and $n = 0.5-0.54$, respectively.

The knowledge of the gel point, in combination with structural observations, allows us to answer questions about the structural state that causes the transition. The structure will be characterized in the following.

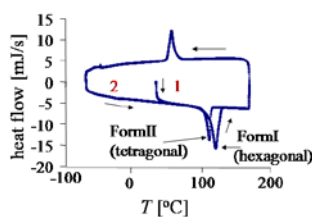


Figure 1. Differential scanning calorimetry for iPB for heating and cooling rates of 10 K/min.

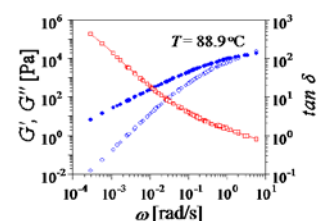


Figure 2. Master curve of iPB melt at crystallization temperature of 88.9 °C.

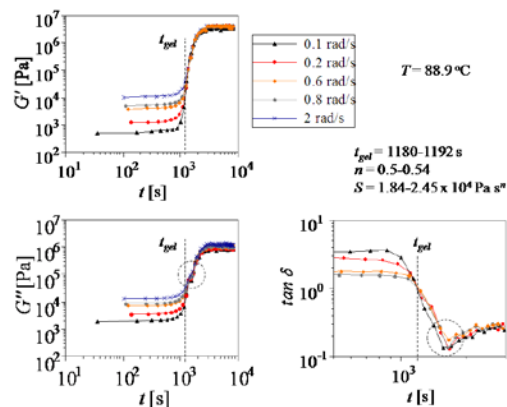


Figure 3. Growth of $G'(t)$ and $G''(t)$ during crystallization of iPB at 88.9°C. The fluid-to-solid transition is marked by the frequency-independent loss tangent. The dip in the loss tangent after the gel point is due to the noisy G'' data, region marked by a circle.

Differential Scanning Calorimetry (DSC). Samples were crystallized isothermally at 88.9 °C. The absolute crystal weight fraction was calculated as $w_{cry}(t) = H(t)/H_{ideal\ crystal}$, where $H(t)$ and $H_{ideal\ crystal}$ are the specific heat evolved up to time 't' for a crystallizing sample and the specific heat required to melt an ideal crystal. We used 146 J/g as heat of melting for an ideal crystal of FormII⁶.

In order to compare amorphous and crystalline domains in the sample, we convert DSC crystal weight fractions (w_{cry}) into crystal volume fractions, $\phi_{cry} = w_{cry} \cdot \rho_{sam} / \rho_{cry}$. We approximate the average sample density, $\rho_{sam} = (\rho_{cry} - \rho_{amo})w_{cry} + \rho_{amo}$, as linear function of the crystal weight fraction; ρ_{cry} (907 Kg/m³) and ρ_{amo} (868 Kg/m³) are densities of the ideal crystal and the amorphous melt, respectively.

The crystal volume fraction (Fig. 4) increases quickly in the first 2500 s, followed by a much slower growth at longer times. The absolute crystallinity (ϕ_{cry}) is normalized with its maximum value ($\phi_{cry, \infty}$). The crystal fraction reaches a value of about 18 vol% at the end of 2500s and further grows slowly to 20 vol%. The absolute crystal volume fraction at the gel point is 7-8 % which is about 1/3 of final crystallinity.

Optical Microscopy. The optical micrograph, Fig. 5, at the gel point shows spherulites of different sizes that are not jammed or packed. Most of them have already impinged whereas others are still

away from impingement. In the micrograph, we observe impingement between pairs of spherulites, though it is hard to define an instant of spherulitic impingement for the whole sample. We find that a percolated structure gives rise to the fluid-to-solid transition rather than jamming or close packing of spherulites. Crystal volume fraction at this instant, from DSC, is 7-8 vol% indicating the amorphous nature of spherulites.

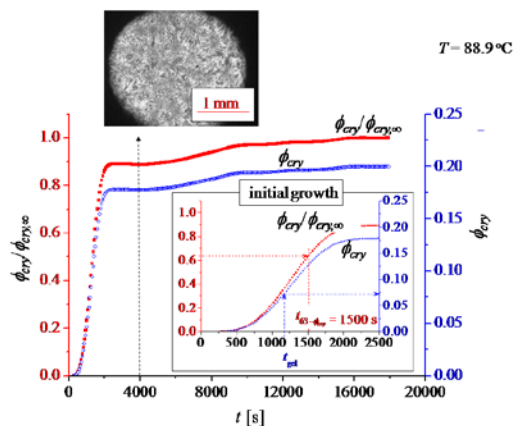


Figure 4. Relative ($\phi_{cry}/\phi_{cry,\infty}$) and absolute (ϕ_{cry}) crystal volume fraction in the entire sample from DSC for isothermal crystallization of iPB at 88.9 °C. The micrograph shows that the sample is already completely filled with spherulites at $t=4000$ s and that further crystal growth has to occur within the primary crystal structure.

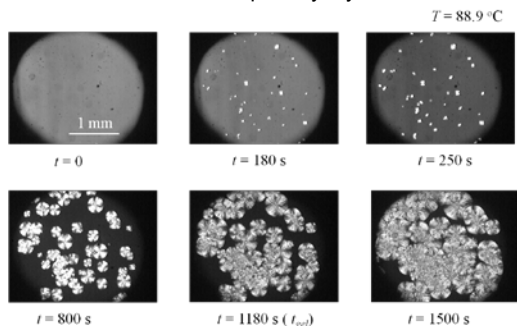


Figure 5. Cross-polar micrographs for crystallizing iPB at 88.9 °C.

DISCUSSION

Dynamic mechanical spectroscopy combined with optical microscopy confirms the percolated nature of structure at the fluid-to-solid transition for crystallizing isotactic poly-1-butene. At the microscopic level, the percolated structure is built by spherulites. The volume fraction of spherulites in the sample is clearly above 50% at the gel point, Fig. 5, though we only found 7-8 vol% crystal that gives rise to sample connectivity. Similar observations were made earlier for crystallizing polymers where fluid-to-solid transition was observed at very low crystal contents ranging from 1-5 vol%⁷. This indicates that spherulites are certainly not equivalent to hard spheres and are mostly amorphous. In addition, due to their growth dynamics, spherulites are expected to be softer at the leading edge than in the interior. Secondary crystallization within a growing spherulite furthers the crystallinity beyond primary crystallization. Thus spherulites are entities with a radial crystal gradient with highest crystallinity in the middle. Crystallization, being an exothermic process, might give rise to higher temperatures locally at the leading edge of spherulites. This might further soften the leading growth front.

Network percolation can be viewed at different length scales. At the length scale of a spherulite, crossing among spherulites can affect the fluid-to-solid transition. Spherulites are formed by branching of sheaf-like crystalline lamellae, which are alike nanosheets. From DSC, we only have 7-8 vol% of such crystalline nanosheets at fluid-to-solid transition. A percolation by these sheets can also lead to sample connectivity. When two neighboring spherulites are about to impinge,

they compete for the same polymer chains and might end up sharing a macromolecular chain, thus forming a bridge molecule for network connectivity at molecular length scale, Fig. 6. We anticipate that a combination of such phenomena, namely spherulite contact/ crossing, percolation among crystal lamellae and bridging molecules between spherulites, leads to network connectivity as required for solidification.

In comparison, a particle volume fraction of 3-4 % is sufficient to enable fluid-to-solid transition in aggregating suspensions². It is interesting to find the same order of magnitude for the crystal volume fraction that enables the fluid-to-solid transition in the semicrystalline polymer.

At the gel point, where $\tan\delta$ becomes independent of frequency (at low probing frequencies), the $\tan\delta$ value is close to unity implying that material is as lossy as it is elastic. Having $\tan\delta$ near 1 at the gel point is exceptional, but it is a permitted value since $\delta=n\pi/2$ depends on the relaxation exponent n which might adopt values in the range $0 < n < 1$ (depending on the specific material of observation). Moduli are in the order of 10^4 Pa.

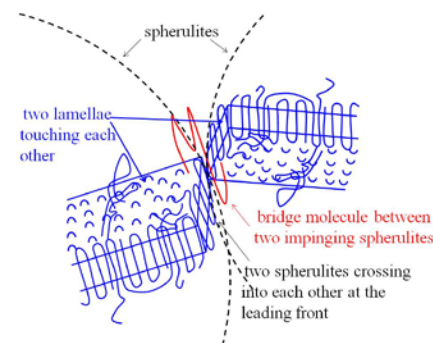


Figure 6. A schematic for a plausible mechanism for crystal connectivity at the interface between two impinging spherulites during crystallization of a semicrystalline polymer- contact and crossing among spherulites, network percolation by crystal lamellae and bridging by molecules.

CONCLUSIONS

Time-resolved mechanical measurements along with crystallinity and morphology help us understand the structure-property relations for crystallizing polymers. It was established that the fluid-to-solid transition takes place due to a percolating network structure, which is constituted of mostly amorphous spherulites. The crossing among spherulites, percolation by crystalline lamellae (nanosheets) and the presence of bridging chains between two spherulites are attributed to the network formation.

ACKNOWLEDGEMENT

We acknowledge NSF for the financial support.

REFERENCES

1. Mours, M.; Winter, H. H. *Rheologica Acta* 1994, 33, 385-397.
2. Xu, X. M.; Tao, X. L.; Gao, C. H.; Zheng, Q. *Journal of Applied Polymer Science* 2008, 107, 1590-1597.
3. Azzurri, F.; Flores, A.; Alfonso, G. C.; Calleja, F. J. B. *Macromolecules* 2002, 35, 9069-9073.
4. Hadinata, C.; Gabriel, C.; Ruellman, M.; Laun, H. M. *Journal of Rheology* 2005, 49, 327-349.
5. Bonn, D.; Coussot, P.; Huynh, H. T.; Bertrand, F.; Debregeas, G. *Europhysics Letters* 2002, 59, 786-792.
6. Kalay, G.; Kalay, C. R. *Journal of Applied Polymer Science* 2003, 88, 814-824.
7. Gelfer, M.; Horst, R. H.; Winter, H. H.; Heintz, A. M.; Hsu, S. L. *Polymer* 2003, 44, 2363-2371.